




Letter

Mapping Mining Areas in the Brazilian Amazon Using MSI/Sentinel-2 Imagery (2017)

Felipe de Lucia Lobo ^{1,2,*} , Pedro Walfir M. Souza-Filho ^{1,3} ,
Evlyn Márcia Leão de Moraes Novo ² , Felipe Menino Carlos ⁴ and
Claudio Clemente Faria Barbosa ⁴

¹ Instituto Tecnológico Vale, Rua Boaventura da Silva, 955, Belém, PA 66055-090, Brazil; pedro.martins.souza@itv.org

² Remote Sensing Division, National Institute for Space Research (INPE), Av. dos Astronautas 1758, São José dos Campos, SP 12227-010, Brazil; evlyn.novo@inpe.br

³ Geosciences Institute, Universidade Federal do Pará, Rua Augusto Correa 1, Belém, PA 66075-110, Brazil

⁴ Image Processing Division, National Institute for Space Research (INPE), Av. dos Astronautas 1758, São José dos Campos, SP 12227-010, Brazil; felipe.carlos@fatec.sp.gov.br (F.M.C.); claudio.barbosa@inpe.br (C.C.F.B.)

* Correspondence: felipe.lobos@inpe.br; Tel.: +55-12-3208-6810

Received: 27 June 2018; Accepted: 20 July 2018; Published: 25 July 2018



Abstract: Although mining plays an important role for the economy of the Amazon, little is known about its attributes such as area, type, scale, and current status as well as socio/environmental impacts. Therefore, we first propose a low time-consuming and high detection accuracy method for mapping the current mining areas within 13 regions of the Brazilian Amazon using Sentinel-2 images. Then, integrating the maps in a GIS (Geography Information System) environment, mining attributes for each region were further assessed with the aid of the DNPM (National Department for Mineral Production) database. Detection of the mining area was conducted in five main steps. (a) MSI (MultiSpectral Instrument)/Sentinel-2A (S2A) image selection; (b) definition of land-use classes and training samples; (c) supervised classification; (d) vector editing for quality control; and (e) validation with high-resolution RapidEye images ($Kappa = 0.70$). Mining areas derived from validated S2A classification totals 1084.7 km² in the regions analyzed. Small-scale mining comprises up to 64% of total mining area detected comprises mostly gold (617.8 km²), followed by tin mining (73.0 km²). The remaining 36% is comprised by industrial mining such as iron (47.8), copper (55.5) and manganese (8.9 km²) in Carajás, bauxite in Trombetas (78.4) and Rio Capim (48.5 km²). Given recent events of mining impacts, the large extension of mining areas detected raises a concern regarding its socio-environmental impacts for the Amazonian ecosystems and for local communities.

Keywords: small-scale mining; industrial mining; google engine; image classification; land-use cover change

1. Introduction

Brazil is one of the leading countries in mineral production, 40% of which comes from the Amazonian states [1] generating large financial compensation for local municipalities and states. At the same time, these activities have profound impacts on the Amazon regional economy, and cause intense social conflicts [2] and environmental impacts, such as water contamination [3]. For example, a recent leak of toxic mining debris discharged by a bauxite mining company has contaminated several communities in Barcarena (Pará State) with high levels of lead, aluminum, sodium, and other toxins detected in drinking water up to 2 km downstream [3]. Another example regards gold exploitation

in the Tapajós River watershed, where water has been contaminated with mercury and impacted by the siltation process due to discharges of artisanal gold-mining tailings since the 1950s [4]. Moreover, recent publications have demonstrated the influence of mining project/activities on the Land Use Cover Change (LUCC) caused by other land-use covers, such as pasture and agribusiness, indicating its importance to territory expansion as well [5,6].

Although mining has an important role for the economy of the Amazon, little is known about its attributes such as area, type, scale, status and socio/environmental impacts. One of the reasons for this absence of information is due the lack of accurate mapping of the mining area [7,8]. This lack is explained by the nature of the mining activity characterized by a diversity of techniques and scale of exploitation. Mining in the Amazon ranges from small-scale with rudimentary techniques (water jets and rafts), more mechanized exploitation with pit loaders and cyanide tanks (in the case of gold extraction) where miners organized themselves into cooperatives, to large-scale mining characterized by high mechanization at an industrial scale (ports, pipelines, roads, etc.) [9,10]. This diversity of techniques and exploitation scale causes different types of land cover, which includes barren soil, land pits, water bodies, degraded and recovering areas [7]. Moreover, a significant amount of small-scale mining occurs in small areas (<10,000 m²) within forest land which are only detectable by medium- to high-resolution images (≤20 m). Therefore, both high spectral variability and high frequency of small-scale mining areas often causes misclassification by image classifiers and interpreters because the visible features of the mines are similar to many other land cover and land-use changes such as clearance for agriculture or cattle farms [8]. Another challenge to map mining areas is that the stream network in which mining takes place can comprise of clear water, but also of highly turbid water and riverbanks, with spectral signatures similar to those of bare soil [8]. One more aspect regarding the criteria for including a given land use to the mining class area is that different land uses such as ports, airstrips, access roads, can be considered to be direct LUCC by mining activities, and therefore added to the exploitation area [7].

Considering all these difficulties and challenges, maps of mining areas are sporadic. To overcome that, research efforts have been made to map mining areas around the world using different remote sensing data and classification methods [11,12]. A recent review article indicates that classification of mining area is improved when using high-resolution imagery and applies machine learning, such as Support Vector Machine (SVM), object-oriented or decision tree to classify mining areas. To detect small-scale mining in Malaysia, for example, some researchers have applied high-resolution imagery [8] and provided high accuracy (89%) maps using object-oriented/SVM classification to detect several mining-related land-cover uses. The high accuracy, however, relied on time-consuming image processing methods. Also, the swath widths of high-resolution images are usually narrow, preventing their application to large-scale areas. For the Brazilian Amazon, the only mining area estimation publicly available is based on visual interpretation of Landsat imagery (30 m) and vector editing (TerraClass Project [13], TC2014). This product, despite the satisfactory location of mining occurrence, lacks details and is subject to misinterpretation. Moreover, due to the use of a time-demanding method, it cannot be updated frequently [12].

Given the economic and environmental importance of mining exploitation around the world, and particularly in the Amazon, the development of rapid and accurate methods for classifying mining areas is key to understanding the influence of mining activities on the regional environment [7]. In this context, this research aims to map current active mining areas (open pits) at a large scale (Brazilian Amazon) and integrate attributes regarding the mining scale and ore exploited. The first objective of this paper is to map current operational mining areas within the main mining regions of the Brazilian Amazon using Sentinel-2A images (S2A) applying a low time-consumption mapping method based on GEE (Google Earth Engine). In the face of a lack of information about the type of mineral exploited and the scale (industrial or small-scale), the second objective is the integration of data provided by Brazilian National Department for Mineral Production—DNPM (license status, mineral type among other information) to the mining map. This integration will be carried out in a GIS (Geographic Information

System) database and will allow computation of the area occupied by each mining category, providing key information for the environmental management of mining activities.

2. Materials and Methods

2.1. Mining Sites in the Brazilian Amazon

Small-scale and large-scale mining are present within numerous regions in the Brazilian Amazon, exploiting several ores such as iron, manganese, bauxite, tin, gold, nickel, and copper. Besides the different ore types, the techniques applied in the exploitation also vary considerably. Industrial iron mining in Carajás, for example, applies high-end technology throughout the whole process of surveying, exploiting, and recovering the area, resulting in high yields with minimum environmental impacts. On the other hand, small-scale gold mining in the Tapajós River, for example, uses low-end technology in ore processing (water jets and dredges) with low yields and high impact levels on land degradation and water contamination (sediment and mercury) [14–17].

To cover the variety of mining activities in the Amazon, 13 main regions for ore exploitation were considered for analysis, including both small-scale and large-scale that present specific characteristics in terms of socio-economic and territorial aspects (Figure 1). The areas were selected based on literature review [10] and other databases [1,13]. Although other areas in the Brazilian Amazon present relevant mining activities, such as the state of Roraima and north of the Amazon State (diamond and gold mining), they were not included either due to the lack of cloud-free images or to the mining process, mainly in rivers in rafts and dredges, which are hardly detectable by satellite imagery [2,18].

Figure 1 shows the study area location and the 38 Sentinel-2A tiles used for mining detection. All the images were selected with data range from July to September 2017, with exception of Taboca (AM) and Serra do Navio (AP), due to a lack of a more recent cloud-free images.

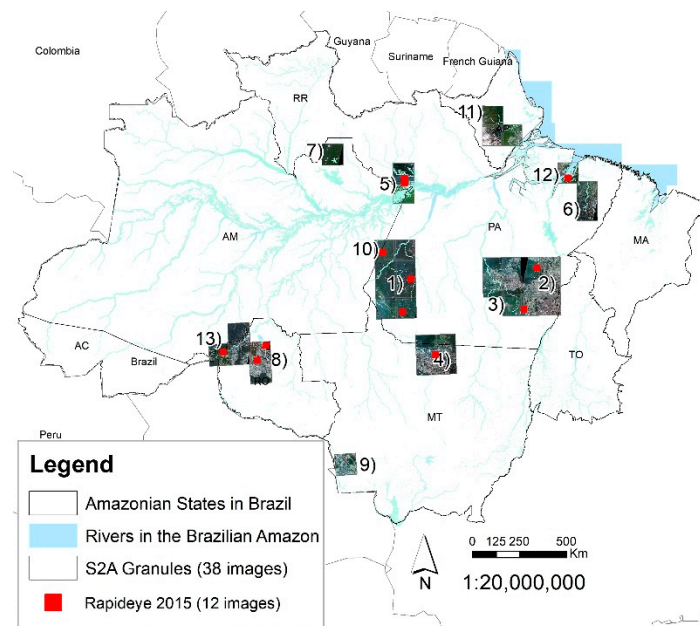


Figure 1. Thirteen mining regions in the Brazilian Amazon evaluated in this study: (1) Tapajós River; (2) Carajás; (3) Rio Xingu; (4) Peixoto de Azevedo; (5) Trombetas/Juruti; (6) Capim River; (7) Mina Taboca; (8) Ariquemes; (9) Pontes e Lacerda; (10) Amanã River; (11) Amapá; (12) Barcarena; (13) Madeira River. Indication of 38 Sentinel-2A images used for mapping mining areas and 12 RapidEye images used for validation purposes. Federal States within the Amazon region: Acre (AC), Amapá (AP), Amazonas (AM), Maranhão (MA), Mato Grosso (MT), Pará (PA), Rondônia (RO), Roraima (RR), and Tocantins (TO).

Based on a literature review [1,13,18], Table 1 provides more general information about each study area including type of ore exploited, Federal Units-State, and whether it is a large-scale (industrial) or small-scale mining (locally called “garimpos”).

Table 1. Information of the mining sites regarding to location, Sentinel-2 tiles and acquisition date, ore exploited and mining scale. Mining scale varies from small-scale (“garimpos” with rudimentary techniques), medium (mines with improved techniques, pitloaders, cyanide tanks), industrial scale (large mining operations with high mechanization which can include ports, pipelines, ore refinery, etc.). Federal Units: AM—Amazonas, AP—Amapá, MT—Mato Grosso, PA—Pará, RO—Rondônia.

#	Mining Sites	F.U.	Sentinel-2 Granule	Date	RapidEye Tile_Date	Ore	Mining Scale
1	Tapajós region	PA	T21 MWQ, MVP, MWP, MVN, MWN, MVM, MWM	19 July 2017	2135416_2015-06-07 2136118_2015-07-23 2136712_2015-07-19	Gold	Small-Medium
2	Carajás region	PA	T22MEU, MFU, MET	13 and 20 July 2017	2235415_2014-07-30 2236318_2015-08-01	Iron, Copper, Manganese, Nickel	Industrial
3	Xingu/Rio Fresco	PA	T22MCU, MDU, MCT, MDT, MET, MDS, MES, MFS	13 and 20 July 2017		Gold/Tin/Nickel	Small/Industrial
4	Teles Pires/Peixoto de Az.	MT	T21LXK, LYK, LXJ, LYJ	6 July 2017	2134423_2015-07-28	Gold	Small-scale
5	Trombetas/Jurutí	PA	T21MWU, MWT	1 December 2017 29 July 2017	2138317_2015-09-21 2138217_2015-09-21	Bauxite	Industrial
6	Rio Capim	PA	T22MHB, MHC	20 July 2017		Kaolinite	Industrial/Pipeline
7	Mina Taboca	AM	T20MRE	3 September 2017		Tin	Industrial
8	Ariquemes region	RO	T20LMQ, LMP	18 and 25 July 2017	2034714_2014-07-28 2034814_2015-07-02	Tin	Small/Industrial
9	Pontes e Lacerda	MT	T20LRJ	19 July 2017		Gold	Small/Industrial
10	Amanã	PA/AM	T21MVQ	19 July 2017		Gold	Small
11	Amapá/Serra do Navio	AP	T22NCF, NCG	18 November 2016		Manganese/Gold	Industrial
12	Barcarena	PA	T22MGD	20 July 2017	2238325_2015-06-28	Bauxite/Kaolinite	Industrial/Port
13	Rio Madeira	RO/AM	T20LLR, LLQ, LKQ	18 and 25 July 2017	2034705_2015-06-24	Gold	Small-scale

2.2. Classification and Validation of Mining Areas

To address the first objective, the mapping process was conducted in five main steps, three of which were carried out in the GEE platform and two in ArcGIS (ESRI, Redlands, CA, USA). In GEE platform:

(a) The first step was to select current (2017) cloud-free images from the Sentinel-2 database within the study areas (Figure 2a). A selection script was applied based on criteria of date and cloud percentage (<20%) to identify the 38 Sentinel-2 granules used (see GEE script at <https://goo.gl/2S8zSp>). The S2A image database available on GEE and used in this study is in digital number (DN) and not submitted to atmospheric correction.

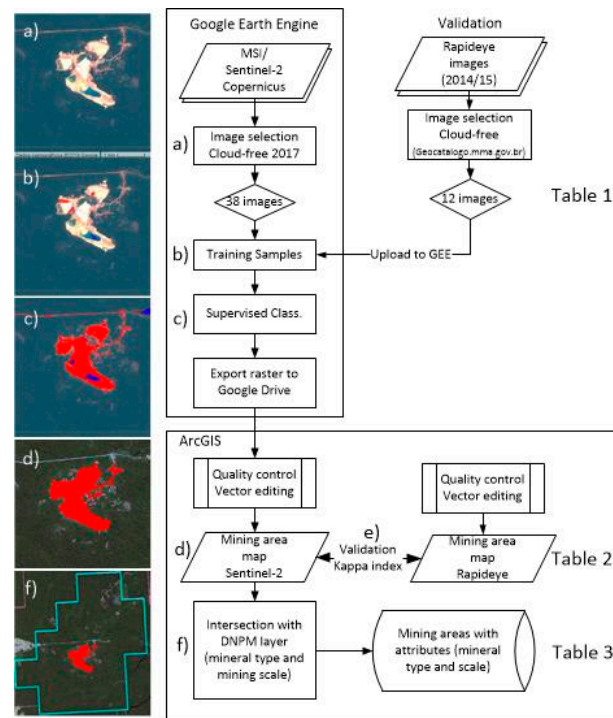


Figure 2. Flowchart with examples of steps taken to address objective 1 (a–e) and objective 2 (f). In GEE (Google Earth Engine): (a) Images selection; (b) training samples; (c) supervised classification followed by exportation. In a Geographical Information System—GIS software: (d) vector editing for quality control, (e) validation of mining areas with RapidEye classification. (f) Identification of mineral type as well as scale by intersecting validated mining map with mining licenses (National Department for Mineral Production—DNPM) layer.

(b) The second step was to define the land-cover classes and select training samples [17]. Initially, four land-use classes were used as reference for the classification process: dense forest, clear-cut deforestation (usually pastures with regular geometry), water bodies and barren soil (open-pit mining areas) (Figure 3a). For each study area, at least 10 small-sized polygons ($\sim 5 \times 5$ pixel) were used as training samples for each class. Although mining areas can include several land-use cover types, the criteria used in this study was to select only currently active areas, i.e., open-pit mining areas that present high albedo levels in comparison to other classes (Figure 3b). The forest class includes dark dense vegetation areas only and for the water class, natural rivers, and lakes, preferentially of low turbidity, were sampled for training process. Clear-cut contains areas of pasture with regular shape with little or non-vegetation (Figure 3a). These classes show spectral difference between each other (Figure 3b). For example, band 4 shows values up to 400 (DN) for water and forest and increased values for clear-cut (1500) and mining (2900), whereas band 6 shows low values for water (200), intermediate level for vegetation (1800) and clear-cut (2000) and high values for mining (3100). The spectral difference among the classes observed allowed proceeding with the classification process.

(c) The third step was to apply a supervised classification available on GEE to the selected images (Figure 3c). The classification method used for mining detection was the Classification and Regression Trees (CART), a non-parametric classifier that does not require any a priori statistical assumptions regarding the distribution of data. Recent research has compared ten machine-learning image classification methods implemented on GEE, such as CART and Random Forest, to map wetlands in Indonesia [19], and indicated that CART presented the mapping accuracy (96%) demonstrating that CART provides reliable outputs for mapping land-use cover. CART is a pixel-based classifier that uses the DN levels from the training samples (polygons) to create a decision tree that classifies each pixel of the image (20 m). Based on Figure 3c, the bands 3 (550 nm), 4 (665 nm), 6 (740 nm), 8 (1600 nm) and

11 (2200 nm) were used by CART to classify S2A imagery into mining, water, forest, and clear-cut areas. To avoid extensive misclassification with inactive mining areas that includes some vegetation mostly where small-scale mining occurs, the mining areas considered for this research included only active mining areas, i.e., barren soil (active exploitation areas) and associated water bodies. Therefore, for the following steps, only the mining and water classes were taken into consideration by removing forest and clear-cut classes from the raster classification (Figure 3c). The resulting layer was exported to Tiff file type into Google Drive. Unfortunately, the export option only provides image exportation up to 1 million pixels, hindering the export of large areas (such as the whole granule extension). This issue is even more relevant in the case of MSI/S2A imagery (10 m). To overcome this issue, the exportation step was conducted with a spatial resolution of 20 m and using subsets to areas of mining occurrence (Region of Interest, ROI).

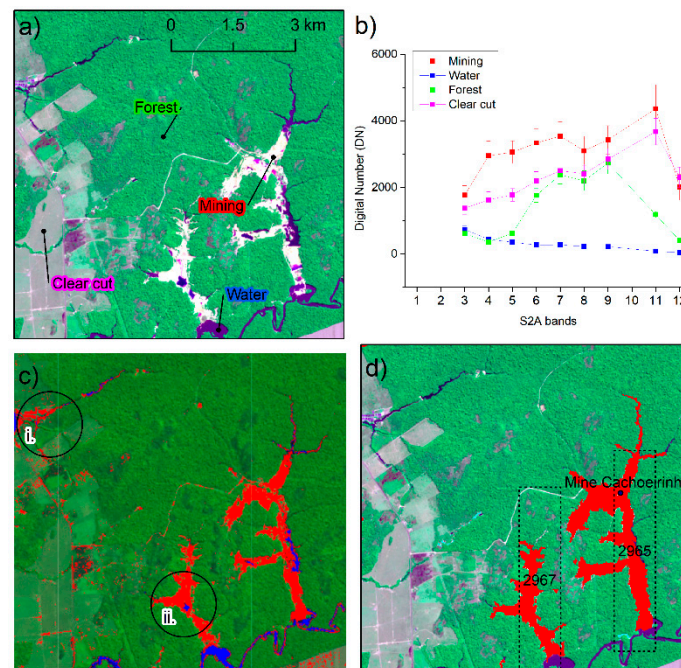


Figure 3. Illustration of the classification process for an industrial mining in Itapuã do Oeste/RO: (a) Sample selection for four classes used (Mining in red, water in blue, forest in green and clear-cut areas in magenta). (b) Average and standard deviation of Sentinel-2A spectra for 25 pixels of each class, bands 1 (443 nm), 2 (490 nm) and 10-Cirrus (1375 nm) were omitted due to high atmospheric effects. (c) Classification result from GEE based on CART (Classification and Regression Trees), only mining areas in red and water areas in blue are shown: (i) indicates commission areas within mining class; and (ii) indicates water bodies derived from mining activities and, therefore, integrated into mining class. (d) Final mining area map after vector edition with indication of Mining License Areas (dashed rectangles) used for type of ore identification (see Table 2 for details on Mining License).

Table 2. Example of information related to the Exploitation License given by DNPM (National Department for Mineral Production). Process numbers refer to the areas indicated in Figure 3d. In this case, two industrial companies have the license to exploit tin in Itapuã do Oeste (RO) with 485 ha each.

Process N.	Year	Area (ha)	Status	Last Update	Name	Ore	Usage	Federal Unit	Municipality
2965	1965	485	Active	6 February 2018	Indústria e Comércio S A	Tin (Sn)	Not informed	RO	Itapuã do Oeste
2967	1965	485	Active	7 February 2018	Ltd.a	Tin (Sn)	Not informed	RO	Itapuã do Oeste

In GIS environment: for data quality control (d), the exported Tiff files, from both S2A and RapidEye classifications, were then collated in a GIS software and submitted to vector editing at 1:25,000 scale to eliminate major miss-classification of mining areas. For example, in Figure 3(c), areas that were committed into mining class were manually removed from vector layer, whereas water bodies that are directly derived from mining operation were re-classified into mining class (Figure 3(cii)). This procedure is dependent on the user's interpretation to distinguish mining areas from those of other uses, which can lead to omission and commission errors (in particular small-scale mining). To support the user's visual interpretation, several ancillary data were used to minimize these errors such as roads, water bodies, limits of gold-mining districts, mining sites and protected areas [7]. This information helped to identify whether barren soil is an open-pit (mining area) or a clear-cut for other land use, for example. Moreover, the capacity of identifying mining areas is more precise using high spatial resolution imagery. Thus, for validation purposes, 12 RapidEye images (5 m) available at geocatalogo.mma.gov.br [20] acquired in 2014/2015 were uploaded to GEE and submitted to the same classification procedure developed for MSI/Sentinel-2 data (Table 1). New independent training samples were selected for each class using RapidEye bands 2 (560 nm), 3 (665 nm), 4 (710 nm) and 5 (805 nm) for CART classification. Although the time gap between S2A 2017 and RapidEye images may introduce commission errors as mining tends to expand from 2015 and 2017, RapidEye is the only high-resolution imagery freely available which can be used for validation. Other high-resolution images, such as Ikonos and WorldView, are available but under purchase only, which would make the mapping very expensive due to the wide extent of the study area.

Therefore, as part of the validation step (e), the results of Sentinel-2 classification (20 m) were compared to the classification derived from RapidEye imagery (5 m), the latter being the reference map (Figure 2e). Digital classification of RapidEye images were resampled to 20 m and used as ground truth for the S2A classification via confusion matrix (Kappa Index). To minimize spatial errors due to georeferencing, all the maps used for validation were projected to UTM (Universal Transverse Mercator) SAD-1969 Brazil coordinate system.

2.3. Identification of Mineral Type and Mining Scale

To address the second objective, validated mining maps derived from S2A images were subject to identification of mineral exploited, mining scale (whether is an industrial or small-scale mining) followed by tabulation of mining area in km². To do so, the validated Mining areas map (2017) was intersected with the territorial mining license layer controlled by Brazilian National Department for Mineral Production (DNPM) [21], which contains information about the mineral, license status and the owner (Figure 2f and Table 2). This information along with ancillary data allowed identification of mineral exploited and scale of mining activities.

3. Results

3.1. Validation of Mining Areas in 2017

In terms of total mining area, even with the time gap of approximately 2 years, both sensors provided quite similar results when examining individual tiles (Figure 4). In terms of map accuracy, Figure 4 shows a better agreement in areas of large-scale mining (>0.70) than those of small-scale mining (<0.70). For example, for Carajás (Figure 4a), characterized by industrial mining activities, Kappa index was 0.86. However, for Tapajós (Figure 4b), containing extensive small-scale mining, the index drops to 0.62. It is interesting to note that for industrial regions, mining concentrated in large areas (presented by few polygons) and in regions dominated by small-scale, a more diffuse land occupation, usually along the river network, was observed. The overall accuracy is above 98%, taking into consideration the 12 RapidEye images (see Table 1) with Kappa index of 0.70 (Table 3).

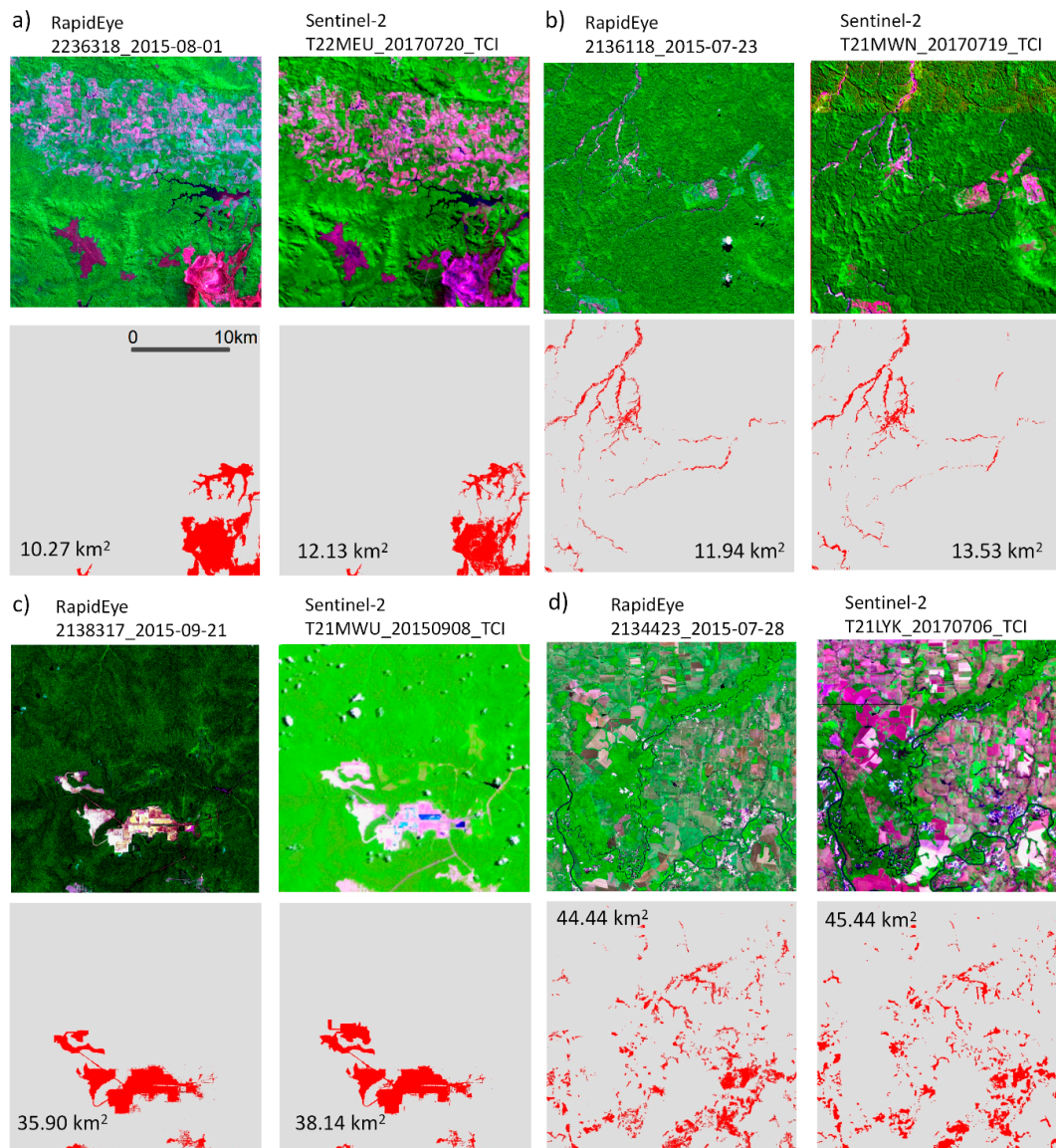


Figure 4. Evaluation of mining classification using S2A images having RapidEye classification maps (25 × 25 km) as ground truth. (a) Carajás region (Industrial), Kappa = 0.86; (b) Tapajós region (Small-scale), Kappa = 0.62; (c) Trombetas region (Industrial), Kappa = 0.87; and (d) Peixoto de Azevedo/Telez Pires region (Small-scale), Kappa = 0.59. RapidEye RGB (3, 5, 2) composition. S2A RGB (4, 8, 3) composition.

Table 3. Confusion matrix of 12 RapidEye tiles and their Sentinel (S2A) equivalent area. Only two classes were considered, mining and not mining areas. Overall accuracy is above 98% and overall Kappa Index is 0.70.

		RapidEye—2014/2015		
		Not	Mining	Total
S2A-2017	Not	7138.63	42.46	6637.09
	Mining	73.17	165.75	238.91
	Total	7218.30	208.20	7426.54

Commission error was larger (73.17 km²) than omission error (42.46 km²) and the total area detected by both imagery data was 165.75 km². The results show that the methodology proposed for S2A data provided satisfactory results, giving support to the analysis of total mining distribution and type of mineral exploited.

3.2. Total Mining Area, Type of Mineral and Mining Scale in 2017

As a result of mining areas derived from S2A images previously validated with RapidEye imagery, a total of 1084.7 km² were mapped considering the 13 regions analyzed. Table 4 shows the total mining area per study area including type of mineral exploited.

Table 4. Mining area in km² mapped with S2A images acquired in 2017 distributed over the study areas and specified by mineral type. For gold and tin, percentage of small-scale mining is shown between brackets. Federal Unit (F.U.).

N	Study Area	F.U.	Gold (% SS)	Tin (% SS)	Baux.	Iron	Cop.	Kaol.	Mang.	Nickel	Sand	Clay	TOTAL (SS%)
1	Rio Tapajós	PA	345.8 (100)										345.8 (100)
2	Carajás	PA	24.2 (100)			47.8	55.1		8.9	4.2	0.7		140.9 (17)
3	Rio Xingu	PA	92.1 (100)	37.8 (100)			2.6			1.9			134.4 (97)
4	Peixoto de A.	MT	116.7 (100)										116.7 (100)
5	Tromb./Juruti	PA			78.4								78.4
6	Rio Capim	PA			48.5			12.2					60.6
7	Mina Taboca	AM		48.8 (0)									48.8 (0)
8	Ariquemes	RO		45.8 (50)									45.8 (50)
9	Pontes e L.	MT	27.7 (50)										27.7 (50)
10	Amanã	AM	27.5 (100)										27.5 (100)
11	Amapá	AP	1.7 (0)			22.1							23.8 (0)
12	Barcarena	PA			12.0			2.3			4.5	0.6	19.4
13	Rio Madeira	RO	1.3 (100)	13.5 (100)									14.8 (100)
	TOTAL (km ²)		637.0 (97)	146.0 (50)	138.9	69.8	57.7	14.5	8.9	6.1	5.2	0.6	1084.7 (64)

The total area exploited by gold mining totals 637.0 km², which is equivalent to 58.7% of the mining area in the Amazon Region. Industrial gold mining takes place in Pontes e Lacerda (13.2 km²) and Amapá (1.7 km²). However, small-scale gold mining is responsible for 97% of the total area distributed over Tapajós (345.8), Peixoto de A. (116.7), Xingu (92.1), Amanã (27.5), Pontes e Lacerda (13.5), and Madeira (1.3 km²). Small-scale also comprises 50% of total tin exploitation, mostly in Rio Xingu (37.8), Ariquemes (22.9), and Rio Madeira (13.5 km²). The remaining 50% of tin mining areas are related to industrial activities in Taboca (48.8) and Ariquemes (22.8 km²). Overall, small-scale mining, including both gold and tin, comprises 64% of total mining area detected.

For the other minerals in Table 4, only industrial mining exploits them. Industrial bauxite mining, for example, takes place in Trombetas (78.4 km²), Rio Capim (48.5 km²) and Barcarena (12.0 km²), totaling 138.9 km². Iron mining is present in Carajás (47.8 km²) and Amapá (22.1 km²), at a total of 69.8 km². Copper is exploited in Carajás (55.1 km²) and Xingu (2.6 km²). Kaolin is exploited at Rio Capim (12.2 km²) and sent by pipeline to Barcarena (2.3 km² of infra-structure). Manganese mining occurs in Carajás only (8.9 km²). For nickel, mining is found in Carajás (4.2 km²) and Rio Xingu (1.9 km²). Sand exploitation is found in Barcarena (4.5 km²) and Carajás (0.7 km²), whereas clay exploitation only occurs in Barcarena (0.6 km²). Figure 5a shows the exploited area per different mining activities.

According to Figure 5, the majority (74%) of the mining areas identified in this study, mostly small-scale gold mining, is within the State of Pará boundaries. In this state, bauxite is the second most exploited mineral, followed by copper, iron, tin and others. For Mato Grosso state, only gold mining was identified, which has 9% out of 144.5 km² as industrial mining. The remaining area is composed of small-scale gold mining. In Rondônia and Amazonas states, tin mining is predominant. However, in Rondônia, tin is exploited equally by small-scale (50%) and industrial mining (50%), whereas in Amazonas only one industrial mining site (Mina Taboca) was identified. In Amapá, a large-scale exploitation of iron comprises most of the mining areas (93%).

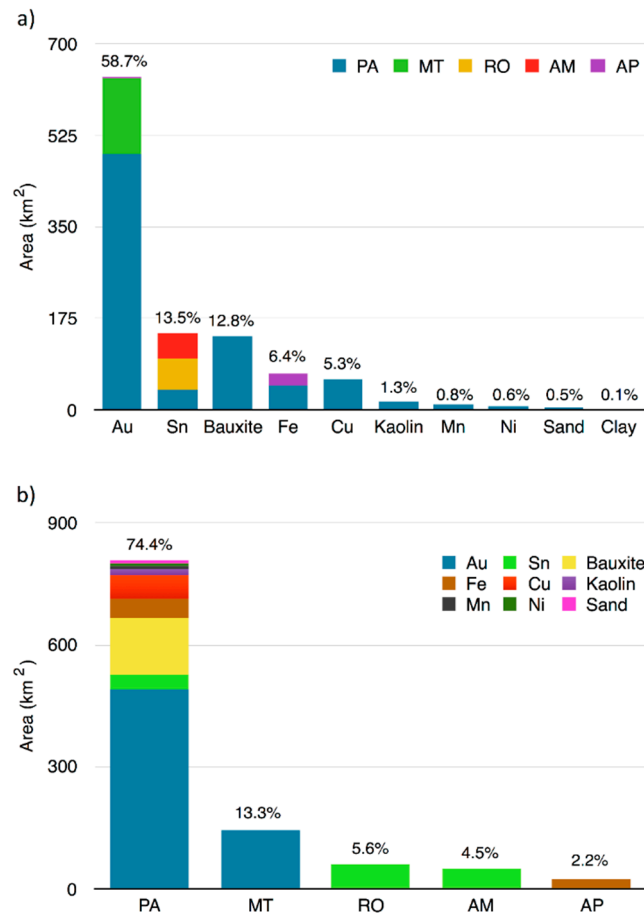


Figure 5. Distribution of mining area (km²) based on mineral types (a): Au—Gold; Fe—Iron; Mn—Manganese; Sn—Tin; Cu—Copper; Ni—Nickel; and Federal Units (b): AM—Amazonas, AP—Amapá, MT—Mato Grosso, PA—Pará, RO—Rondônia.

4. Discussion

4.1. Method for Mapping Mining Areas and Constrains

Considering that the only mining area estimation for the Brazilian Amazon currently available is based on visual interpretation (TC2014), the first contribution of this research was to develop a cost-effective method, in terms of time and resources, to map mining areas in the Brazilian Amazon with satisfactory performance. Created in GEE environment, the mapping process allows quick access and selection of S2A images, which usually would take hours for selecting and downloading S2A images from the usgs.gov database for example, can be now done in minutes [22]. In addition, the classification step is much faster than on stand-alone image processing. For example, in the cloud (GEE) a supervised classification takes a few seconds, whereas in GIS software it usually takes several minutes or hours, depending on the computer configuration. Finally, employing the GEE for the classification suffers from the limitation of restricting the size of exports and thus, preventing the exportation of large areas in 10 m resolution.

On the other hand, the use of CART to classify mining areas presented some issues. Because CART is a pixel-based algorithm, some mining areas were not fully classified, leaving isolated pixels within a mining area, for example. One way to minimize it was to apply a low-pass filter in GIS environment. Another issue regards commission errors. Even though a careful selection of training samples were conducted for four main classes, i.e., mining (open-pits), water (natural water bodies), forest (dense dark vegetation) and clear-cut (pasture with regular shape), commission errors were

often identified, mostly commissions of barren soil of other land-cover uses, such as pasture (Figure 3c). Given the high spectral variability of mining areas (barren soil, water, recovery areas, etc.) [7], a refined evaluation of what areas/polygons were or were not mining areas was necessary based on ancillary information to improve the map precision. The use of ancillary data such as mining sites, mining license, information about other land-cover uses (such as aquaculture, cattle regions, agriculture) as well as literature review was fundamental to identify the main mining areas, and is encouraged to be used on research for mining area detection. Therefore, a fully automatic method that detects mining areas with high precision is yet to be developed. Overall, the method presented here shows a progress toward a quick and accurate method for mining detection in large scale, such as the Brazilian Amazon.

4.2. Validation of Mining Areas with RapidEye Imagery

Besides being a quick method for mapping mining areas, the accuracy between mining maps derived from S2A in comparison to those from RapidEye confirms that the proposed method provides satisfactory results. As shown in Figure 4, the accuracy is higher among large-scale areas than for small-scale mining. The difference in Kappa index occurs because of two reasons: (1) the more concentrated mining areas in industrial mining allows easier detection in comparison to small-scale where a diffuse distribution of small polygons is observed; (2) Also, on small-scale, the LUCC is more dynamic, expanding or recovering quicker than industrial activities. Therefore, in the case of a 2-year gap, the commission error is more likely to occur.

The mining detection improvement using the proposed methods is more evident when we compared the currently available mining areas (TC2014 database) to RapidEye classification (2014/2015) used as ground truth (Figure 6).

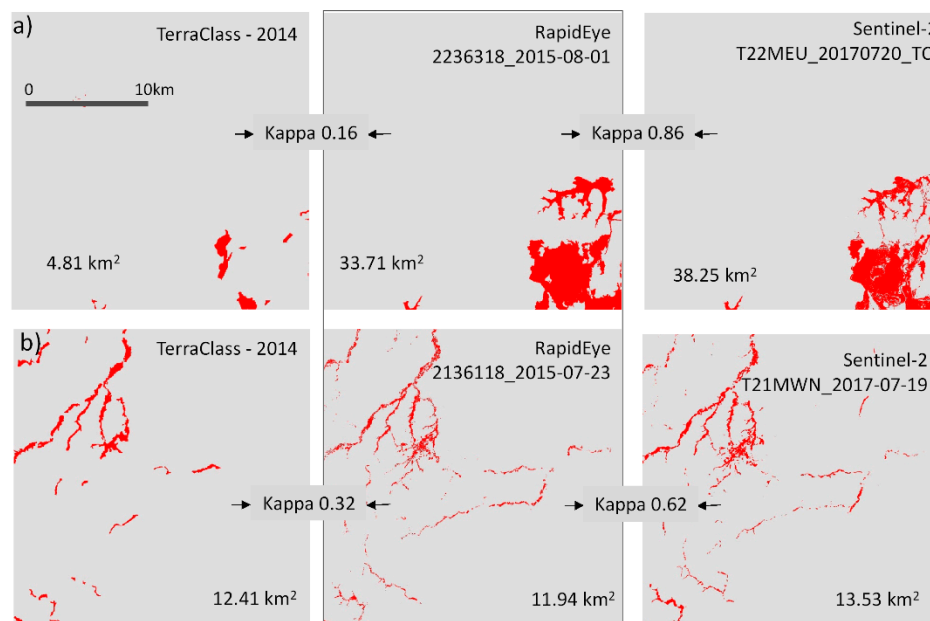


Figure 6. Comparison of mining areas between current available data (TerraClass 2014), map from RapidEye (taken as ground truth and limited to validation tiles, 25 × 25 km) and Sentinel-2A (mining maps for all study areas). In Carajás region (a), accuracy measured by Kappa index shows an improvement from 0.16 (TC2014) to 0.86 (S2A), due to a large omission error in TC2014. For small-scale mining in Tapajós (b), Kappa increased from 0.32 to 0.62. S2A classification were able to detect small polygons, whereas TC2014, due to a coarser classification, lacks detail.

For industrial mining in Carajás, for example, TC2014 detected only 4.81 km², resulting in a weak agreement with RapidEye classification (Kappa = 0.16), whereas S2A classification showed a Kappa index of 0.86. In the case of small-scale in Tapajós, the total area among all classifications were similar

but the TC2014 classification lacks in detecting very small polygons (Figure 6). The lack of details in TC2014 maps can be attributed to (1) misclassification during visual interpretation and (2) to a lower spatial resolution (30 m) of Landsat images used for TC2014 maps, as compared to RapidEye (5 m) and Sentinel-2 (20 m) used in this study.

4.3. Total Area, Type of Mineral and Scale

The second main contribution of this research is the identification of scale and mineral type for each mining area mapped. According to Table 4, some minerals such as iron, manganese, copper, and nickel are exploited by industrial mining only, even though it comprises approximately a third of the total mining area mapped in this research. Industrial mining in the Brazilian Amazon is responsible for approximately 14% of total national annual exportation [1]. For some minerals such as bauxite, copper, kaolin, manganese and tin, Amazonian production totals 90% of national production. To illustrate its economic importance, the Financial Compensation for Mining Exploitation [1] indicates that incomes from Amazonian mining exportation yielded, approximately, US\$ 531 million in 2016, of which 96% are related to the state of Pará, mostly from iron, bauxite and copper exploitation, which corresponds to 90% of total exportation in Pará.

While industrial mining has a significant financial importance and usually follows legal procedures for mining exploitation and the commitment of recovering degraded areas, several socio-environment impacts have recently been reported. For example, water contamination by bauxite exploitation in Barcarena [3], and by nickel exploitation in the Cateté river nearby Xikrin Indigenous Land [4].

Table 4 also shows that mining areas in the Brazilian Amazon is mostly occupied by small-scale gold mining, in particular Tapajós, Xingu/Fresco and Peixoto de Azevedo (MT). Including tin mining, small-scale comprises up to 64% of total mining area detected in this study. According to Enriquez [18], approximately 150,000 people are directly involved in small-scale mining in the Brazilian Amazon. This activity creates a large amount of income (~US\$ 10 million per month for the regional economy [2]) which is rarely subject to taxes or control because most of the area is informally or illegally installed.

The large extension of small-scale mining raises a concern regarding its socio-environment impacts for the Amazonian ecosystems and for local people, since it usually does not follow environmental protocols to recover degraded areas. In fact, recent studies have demonstrated the impact of small-scale gold mining in the Tapajós River and its tributaries (Crepuri, Novo and Tocantinzinho rivers) where intense water siltation occurs [12,16,17]. The impacts also include geomorphological changes in the riverbed and landscapes, causing severe impacts on benthic [23] and fish communities [24–27], not to mention the mercury contamination used in the gold amalgamation process [24,28–30] which is usually illegally imported [31].

5. Conclusions

This research presents a quick and efficient classification method developed in GEE to map mining areas in the Brazilian Amazon. The methods rely on quick access to S2A database, supervised classification of mining and other land-cover uses, exportation to GIS software, followed by vector editing to assure the product's quality control. Besides reducing image processing time, the methods provided accurate maps when compared to classifications derived from high-resolution RapidEye imagery (overall Kappa equals 0.70).

The main novelty of this research is the identification of scale and mineral type for each mining area mapped. Based on this identification, we concluded that small-scale mining (gold and tin) comprises up to 64% of total mining area detected in this study, which raises a concern regarding its socio-environment impacts for the Amazonian ecosystems and for local people, since it usually does not follow environmental protocols to recover degraded areas. The remaining 36% of mining areas in the Brazilian Amazon is comprised of industrial mining, which is responsible for most iron, manganese, copper, and nickel production. While industrial mining has a significant financial

importance and usually follows legal procedures for mining exploitation and the commitment of recovering degraded areas, several socio-environment impacts have recently been reported and are raising a concern regarding its socio-environment impacts.

Given the satisfactory results, the methods presented here will be applied to map deforestation far beyond operational mining boundaries. Furthermore, we will carry out a historical mapping from satellite images, such as Landsat, to support further investigation of water quality and on LUCC in areas under the influence of both industrial and small-scale mining in the Brazilian Amazon.

Author Contributions: F.d.L.L. participated in every step of this article from planning, data processing, analysis, and writing the manuscript as the first author. P.W.M.S.-F. and E.M.L.d.M.N. were the co-supervisors of this research and were fundamental to define the research approach and data analysis. F.M.C. developed the GEE script and C.C.F.B., head of LabISA (The Instrumentation Laboratory for Aquatic Systems) where this research was conducted, collaborated with the methodological approach.

Funding: This research was funded by Coordenação de Aperfeiçoamento de Pessoal de Nível Superior (CAPES, Brazil) and Instituto Tecnológico da Vale (ITV, Brazil), Project ‘Uso Sustentável de Recursos Naturais em Regiões Tropicais’ (15024016001P1), as a Post-PhD Fellowship for F.d.L.L. Trainee Scholarship for F.M.C. funded by CNPq (Brazilian National Council for Scientific and Technological Development, Process: 135114/2017-9).

Acknowledgments: Research developed in a partnership between the ITV (Instituto Tecnológico da Vale) and INPE (Instituto Nacional de Pesquisas Espaciais) in Brazil. We would like to thank both reviewers for their insightful comments, which enabled us to improve the paper. Thanks to Lauren Pansegrouw for English revision.

Conflicts of Interest: The authors declare no conflict of interest.

References

1. Pinheiro, W.F.; Ferreira Filho, O.B.; Neves, C.A.R. *Anuário Mineral Brasileiro: Principais Substâncias Metálicas*; DNPM: Brasília, Brazil, 2016; p. 31.
2. Fernandes, F.R.C.; Alamino, R.d.C.J.; Araújo, E.R. *Recursos Minerais e Comunidade: Impactos Humanos, Socioambientais e Econômicos*; CETEM/MCTI: Rio de Janeiro, Brazil, 2014; Volume 1.
3. Nathanson, M. Norsk Hydro Accused of Amazon Toxic Spill, Admits ‘Clandestine Pipeline’. *Mongabay*, 27 February 2018. Available online: <https://news.mongabay.com/2018/02/norsk-hydro-accused-of-amazon-toxic-spill-admits-clandestine-pipeline/> (accessed on 5 June 2018).
4. Hofmeister, N.; Silva, J.C.D. The River is Dead: Is a Mine Polluting the Water of Brazil’s Xikrin Tribe? *Guardian*. 2018. Available online: <https://www.theguardian.com/global-development/2018/may/15/brazil-xikrin-catete-river-amazon> (accessed on 18 May 2018).
5. Sonter, L.J.; Herrera, D.; Barrett, D.J.; Galford, G.L.; Moran, C.J.; Soares-Filho, B.S. Mining drives extensive deforestation in the Brazilian Amazon. *Nat. Commun.* **2017**, *8*, 1013. [[CrossRef](#)] [[PubMed](#)]
6. Sonter, L.J.; Moran, C.J.; Barrett, D.J.; Soares-Filho, B.S. Processes of land use change in mining regions. *J. Clean. Product.* **2014**, *84*, 494–501. [[CrossRef](#)]
7. Chen, W.; Li, X.; He, H.; Wang, L. A review of fine-scale land use and land cover classification in open-pit mining areas by remote sensing techniques. *Remote Sens.* **2017**, *10*, 15. [[CrossRef](#)]
8. Isidro, C.; McIntyre, N.; Lechner, A.; Callow, I. Applicability of earth observation for identifying small-scale mining footprints in a wet tropical region. *Remote Sens.* **2017**, *9*, 945. [[CrossRef](#)]
9. Veiga, M.M.; Hinton, J.J. Abandoned artisanal gold mines In the Brazilian Amazon: A legacy of mercury pollution. *Nat. Res. Forum* **2002**, *26*, 15–26. [[CrossRef](#)]
10. Cuchierato, G. 200 maiores minas brasileiras. *Minérios & Minerales*, November/December 2016; p. 45.
11. Garai, D.; Narayana, A.C. Land use/land cover changes in the mining area of Godavari coal fields of Southern India. *Egypt. J. Remote. Sens. Space Sci.* **2018**. [[CrossRef](#)]
12. Lobo, F.; Costa, M.; Novo, E.; Telmer, K. Distribution of artisanal and small-scale gold mining in The Tapajós River Basin (Brazilian Amazon) over the past 40 years and relationship with water siltation. *Remote Sens.* **2016**, *8*, 579. [[CrossRef](#)]
13. Almeida, C.A.D.; Coutinho, A.C.; Esquerdo, J.C.D.M.; Adami, M.; Venturieri, A.; Diniz, C.G.; Dessay, N.; Durieux, L.; Gomes, A.R. High spatial resolution land use and land cover mapping of the Brazilian Legal Amazon in 2008 using landsat-5/tm and modis data. *Acta Amazon.* **2016**, *46*, 291–302. [[CrossRef](#)]

14. Coelho, M.C.N.; Wanderley, L.J.; Costa, R.C. Small scale gold mining in the xxi century. Examples in the south-west brazilian amazon. *Anuário do Instituto de Geociências-UFRJ*. **2016**, *39*, 5–14. [[CrossRef](#)]
15. Monteiro, M.D.A.; Coelho, M.C.N.; Cota, R.G.; Barbosa, E.J.D.S. Ouro, empresas e garimpeiros na amazônia: O caso emblemático de Serra Pelada. *Revista Pós Ciências Sociais-UFMA (Universidade Federal do Maranhão)* **2010**, *7*, 28.
16. Lobo, F.; Costa, M.; Novo, E.; Telmer, K. Effects of small-scale gold mining tailings on the underwater light field in the Tapajós River Basin, Brazilian Amazon. *Remote Sens.* **2017**, *9*, 861. [[CrossRef](#)]
17. Lobo, F.L.; Costa, M.P.F.; Novo, E.M. Time-series analysis of Landsat-MSS/TM/OLI images over Amazonian waters impacted by gold mining activities. *Remote Sens. Environ.* **2015**, *157*, 170–184. [[CrossRef](#)]
18. Enríquez, M.A. Mineração na Amazônia. *Parcerias Estratégicas*. **2014**, *19*, 155–198.
19. Farda, N.M. Multi-temporal land use mapping of coastal wetlands area using machine learning in Google Earth Engine. *IOP Conf. Ser. Earth Environ. Sci.* **2017**, *98*, 012042. [[CrossRef](#)]
20. MMA. *Geocatalogo Mma-Rapideye Imagery*; MMA: Brasília, Brazil, 2018. Available online: <http://geocatalogo.mma.gov.br/index.jsp> (accessed on 14 February 2018).
21. Departamento Nacional de Produção Mineral (DNPM). *Sistema De Informações Geográficas Da Mineração-Sigmine*; DNPM: Brasília, Brazil, 2018; Volume 1. Available online: <http://sigmine.dnpm.gov.br/webmap/> (accessed on 20 February 2018).
22. Parente, L.; Ferreira, L. Assessing the spatial and occupation dynamics of the Brazilian pasturelands based on the automated classification of MODIS images from 2000 to 2016. *Remote Sens.* **2018**, *10*, 606. [[CrossRef](#)]
23. Couceiro, S.R.M.; Hamada, N.; Forsberg, B.R.; Padovesi-Fonseca, C. Trophic structure of macroinvertebrates in Amazonian streams impacted by anthropogenic siltation. *Austral Ecol.* **2011**, *36*, 628–637. [[CrossRef](#)]
24. Nevado, J.J.B.; Martin-Doimeadios, R.C.R.; Bernardo, F.J.G.; Moreno, M.J.; Herculano, A.M.; do Nascimento, J.L.M.; Crespo-Lopez, M.E. Mercury in the Tapajós River Basin, Brazilian Amazon: A review. *Environ. Int.* **2010**, *36*, 593–608. [[CrossRef](#)] [[PubMed](#)]
25. Sampaio da Silva, D.; Lucotte, M.; Paquet, S.; Davidson, R. Influence of ecological factors and of land use on mercury levels in fish in the Tapajós River Basin, Amazon. *Environ. Res.* **2009**, *109*, 432–446. [[CrossRef](#)] [[PubMed](#)]
26. Dorea, J.G.; Barbosa, A.C. Anthropogenic impact of mercury accumulation in fish from the Rio Madeira and Rio Negro rivers (amazonia). *Biol. Trace Element Res.* **2007**, *115*, 243–254. [[CrossRef](#)] [[PubMed](#)]
27. Boudou, A.; Maury-Brachet, R.; Coquery, M.; Durrieu, G.; Cossa, D. Synergic effect of gold mining and damming on mercury contamination in fish. *Environ. Sci. Technol.* **2005**, *39*, 2448–2454. [[CrossRef](#)] [[PubMed](#)]
28. Rabitto, I.d.S.; Bastos, W.R.; Almeida, R.; Anjos, A.; de Holanda, Í.B.B.; Galvão, R.C.F.; Neto, F.F.; de Menezes, M.L.; dos Santos, C.A.M.; de Oliveira Ribeiro, C.A. Mercury and ddt exposure risk to fish-eating human populations in Amazon. *Environ. Int.* **2011**, *37*, 56–65. [[CrossRef](#)] [[PubMed](#)]
29. Coelho-Souza, S.A.; Guimarães, J.R.D.; Miranda, M.R.; Poirier, H.; Mauro, J.B.N.; Lucotte, M.; Mergler, D. Mercury and flooding cycles in the Tapajós River Basin, Brazilian Amazon: The role of periphyton of a floating macrophyte (*paspalum repens*). *Sci. Total Environ.* **2011**, *409*, 2746–2753. [[CrossRef](#)] [[PubMed](#)]
30. Telmer, K.; Veiga, M. Chapter 6: World Emissions of Mercury from Artisanal and Small Scale Gold Mining. In *Mercury Fate and Transport in the Global Atmosphere*; Pirrone, N., Mason, R., Eds.; Springer Science, Switzerland AG: Basel, Switzerland, 2009; pp. 131–172.
31. NSCTV. Operacao faz apreensao de Carga de Mercurio no Porto de Itajai. 2018. Available online: <https://g1.globo.com/sc/santa-catarina/noticia/operacao-faz-apreensao-de-carga-de-mercurio-no-porto-de-itajai.ghtml> (accessed on 12 June 2018).

